ORIGINAL

Sediment deposition in the central Hauraki Gulf, New Zealand

Florian Boxberg[1] · Brice Blossier[1] · Willem P. de Lange[2] · Bethany Fox[3,2] · Dierk Hebbeln[1]

Abstract

Based on the analysis of 14 short sediment cores, we present new insights into the distribution of surficial sediments in the central Hauraki Gulf, a semi-enclosed coastal embayment on the northeast coast of New Zealand's North Island. We identify and discuss the effects of interaction of modern wind-generated waves and currents with regard to deposition and reworking of sediments in the Gulf. The modern hydrodynamic regime is controlled by tidal currents, oceanic inflows, and wave-induced currents and it is responsible for a N-S gradient in sediment texture and elemental concentrations in the central Hauraki Gulf sediments. The present-day sediment input into the system is generally low and consists of fine-grained fluvial sediments mostly deposited in the southern study area and comparatively high inputs of relict carbonate material to the northern study sites. The central Hauraki Gulf sediments, which show numerous age reversals in the sedimentary record, can be characterised as palimpsest sediments, as a consequence of continuous reworking and storm-induced sediment transport. In view of the new data, a previously assumed significant post-transgression accumulation of sediments of > 10 m in the central Hauraki Gulf appears to be very unlikely.

Introduction

In recent times, the management, conservation, and sustainable use of near-coastal marine ecosystems have become increasingly important due to the ongoing anthropogenic modification and utilisation of these ecosystems (e.g. Waycott et al. 2009). The conservation of pristine coastal marine ecosystems or the restoration of anthropogenically modified ecosystems is a particularly important issue in highly populated areas with severe human impacts such as the runoff of pollutants and nutrients into coastal waters (e.g. Howarth et al. 2000; Smith 2003). The sustainable use of these ecosystems requires a detailed knowledge of the seafloor setting and the processes controlling it.

The Hauraki Gulf, a shallow and semi-enclosed coastal embayment on the northeast coast of the North Island of New Zealand (Fig. 1), is an example for such a near-coastal

marine ecosystem. It has been affected by anthropogenic activities since the arrival of the Polynesian settlers (~ 1000 year BP) and probably more profoundly since the early European settlement in the area (~ 1800 AD) (e.g. Bussell 1988; McGlone and Wilmshurst 1999). The Gulf plays an important role for New Zealand because it (i) covers the largest shelf embayment of New Zealand and (ii) borders the largest population centre of New Zealand, Auckland, and hence is important for both commercial and recreational activities for approximately one-third of New Zealand's population. Even though the Gulf has been subject to a large number of studies (e.g. Hume et al. 2000, Black et al. 2000, Zeldis et al. 2004, Manighetti and Carter 1999), the seafloor setting and the processes controlling it have only partly been investigated and are not yet fully understood. For instance, there is some dispute in the literature concerning the processes controlling sedimentation patterns in the Gulf. Two main conceptual models have been proposed: a conceptual model of partly event-driven near-bed sediment transport (Manighetti and Carter 1999), and a numerical model invoking "normal" residual or net circulation patterns in the Gulf as the dominant control (Proctor and Greig 1989). These two models would result in different sedimentation patterns, but the extent to which either is accurate in the central Hauraki Gulf is not known.

Through analysis of 14 short sediment cores retrieved from the central Hauraki Gulf, this study aims to (i) improve the understanding of surficial sediment distribution in the central

✉ Dierk Hebbeln
dhebbeln@marum.de

[1] MARUM - Center for Marine Environmental Sciences, University of Bremen, Bremen, Germany

[2] School of Science, University of Waikato, Hamilton, New Zealand

[3] Department of Biological and Geographical Sciences, University of Huddersfield, Huddersfield, UK
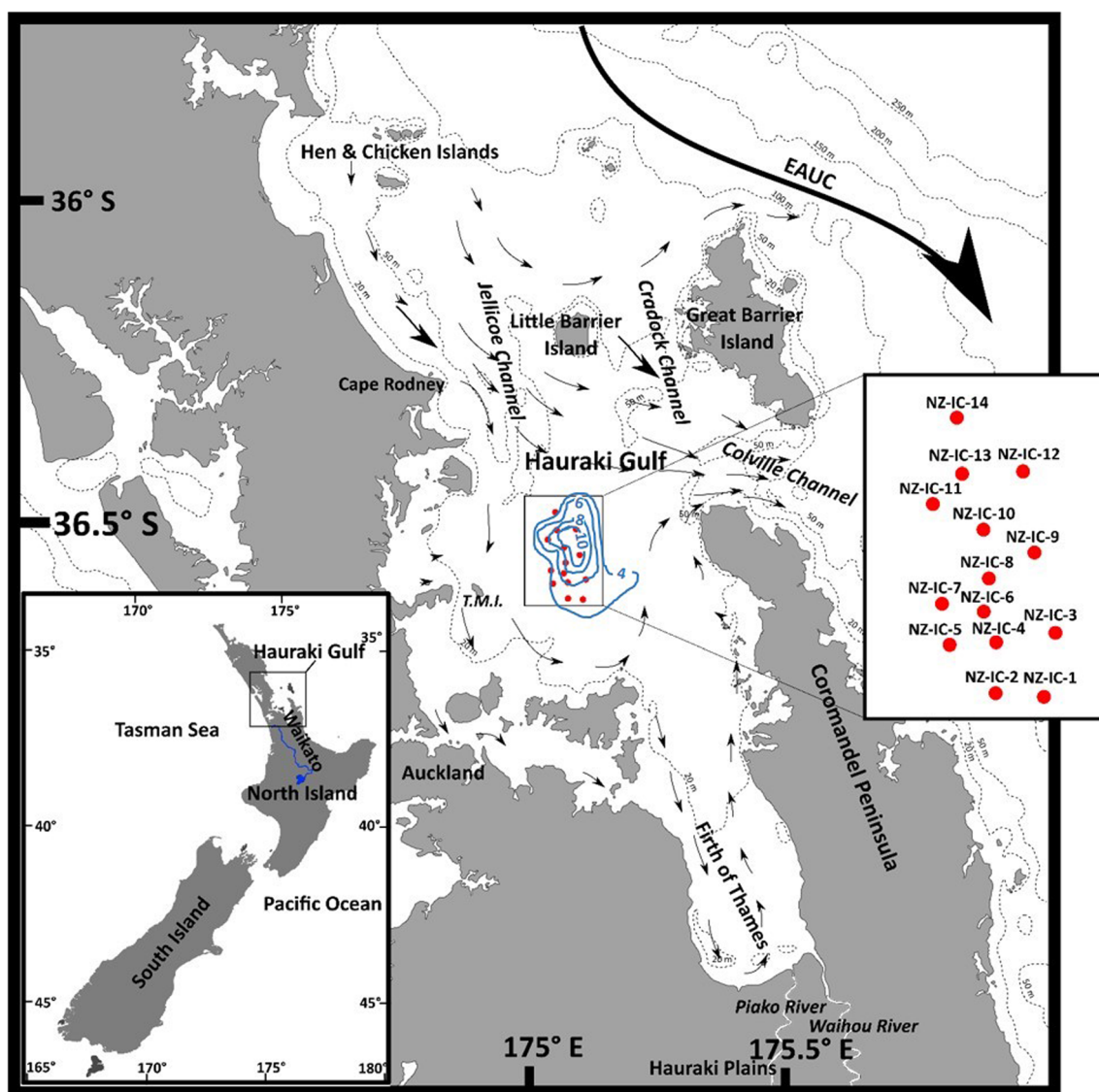
Fig. 1 Location of the study area in the Hauraki Gulf. The left inset map shows the study area on the North Island of New Zealand and the present course of the Waikato River. Red dots in the main map mark the core locations (NZ-IC-1 to NZ-IC-14; right inset map). Blue isolines indicate the proposed thickness of the post-transgressive sediment thickness (m) in the sampling area according to Manighetti and Carter 1999. Black arrows indicate the prevailing surface currents in and outside the Gulf according to Black et al. (2000) (T.M.I.—Tiritiri Matangi Island; EAUC—East Auckland Current)

Hauraki Gulf and (ii) identify and discuss the effects of the interaction of wind-generated waves and currents with respect to deposition and reworking of sediments in the Gulf. Thereby, it will assess which of the two conceptual models (Proctor and Greig 1989; Manighetti and Carter 1999) mentioned above has the greatest influence on sediment deposition in this region.

Regional setting

The Hauraki Gulf is bounded to the east by the Coromandel Peninsula, to the south by the Hauraki Plains and to the west by the Auckland region. To the north, it is partially open to the Pacific Ocean (Fig. 1). Water depths in the Gulf increase northwards, with depths of < 40 m in the inner Gulf south of Tiritiri Matangi Island, 40–50 m in the central Gulf between Tiritiri Matangi Island and Cape Rodney, and 50–100 m north of Cape Rodney to the Hen and Chicken Islands (Fig. 1). The southern end of the Hauraki Gulf consists of the wide and relatively shallow Firth of Thames with water depths < 20 m (Manighetti and Carter 1999). The Gulf has been subject to a broad range of studies covering aspects such as sediment distribution (e.g. Eade 1974; Carter and Eade 1980; Greig 1982; Manighetti and Carter 1999), water circulation within the Gulf (e.g. Greig and Proctor 1988; Proctor and Greig 1989; Greig 1990; Black et al. 2000; Zeldis et al. 2004), geophysical investigation of sub-seabed structures (e.g. Hochstein and

Nixon 1979; Hochstein et al. 1986; Thrasher 1986), organic matter distribution (e.g. Uhle et al. 2007; Sikes et al. 2009), and paleoenvironmental analyses (Greig 1982; Pocknall et al. 1989).

Sediments in the Hauraki Gulf

The seafloor in the Hauraki Gulf is characterised as a smooth and flat surface (Manighetti and Carter 1999). Sediments in the sheltered Firth of Thames (Fig. 1) are predominantly fine grained, consisting of sandy and calcareous mud (Eade 1974; Carter and Eade 1980; Greig 1982). Towards the north, sediments generally become coarser, ranging from sandy mud to muddy sand. However, the presence of finer sediments in more sheltered areas has been interpreted to reveal a dominant wave and current rather than a depth control on the grain-size distribution (Sikes et al. 2009).

Modern-day terrigenous input is low (estimated to 0.35 to 0.82 MT year^{-1}; Griffiths and Glasby 1985; Hicks et al. 2011), consisting of mud and fine sands supplied by several small rivers (Manighetti and Carter 1999). The bulk of the terrigenous sediment is trapped within estuaries and sheltered embayments such as the Firth of Thames (Carter and Eade 1980; Greig 1982). Nevertheless, for the central Hauraki Gulf, the thickness of sediment deposited since the Holocene marine transgression has been estimated by Manighetti and Carter (1999) to be up to 12 m within relatively confined depocenters (Fig. 1). After the last glacial period, the deglacial marine transgression reached the outer shelf at ~ 15 ka B.P. (Carter et al. 1986). The study area, with present-day water depths of ~ 45 m, was inundated by the rising sea level between 12 and 9.5 ka B.P. (Carter et al. 1986) and present-day sea level was reached at approximately 8.1–7.3 ka B.P. (Clement et al. 2015). Subsequently, sea level continued to rise, reaching a high-stand up to 2 m above present at ~ 4 ka B.P. before falling to the present-day levels at ~ 1 ka B.P. (Dougherty and Dickson 2012).

Prior to ~ 24 ka BP, the sedimentary history of the Hauraki Gulf was strongly connected to the Waikato River (Manville and Wilson 2004; Fig. 1), presently New Zealand's longest river with a total length of ~ 425 km. The Waikato River, draining the central volcanic region of New Zealand's North Island, was the major supplier of sediments to the Hauraki Gulf over much of its history. However, at ~ 24 ka B.P., the river changed its course: where previously it flowed into the Hauraki Gulf or the corresponding alluvial plains under lower-than-present sea-level conditions, it now flows into the Tasman Sea (Manville and Wilson 2004). Based on mineralogical data, it has been suggested that a significant proportion of the coastal sands found presently along the western side of the Hauraki Gulf were derived by reworking and onshore movement of older Waikato River deposits on the continental

shelf during the last major marine transgression (Schofield 1970).

Circulation in the Hauraki Gulf

Water exchange between the Gulf and the Pacific Ocean takes place through three major channels: Jellicoe Channel between Little Barrier Island and the mainland (Cape Rodney), Cradock Channel between Great Barrier Island and Little Barrier Island, and Colville Channel between Great Barrier Island and the northern tip of the Coromandel Peninsula (Fig. 1). Water circulation and currents in the Hauraki Gulf are driven by the interaction of tidal flows and the seafloor topography, which concentrates flow through the channels, and by winds creating pressure gradients within the Gulf, which vary in strength with wind direction and magnitude (Black et al. 2000).

In general, water enters the Gulf through Jellicoe Channel, flows anti-clockwise across the central/inner Gulf, and leaves the Gulf via Colville Channel (Greig 1990; Fig. 1). Waters entering the Gulf through Cradock Channel usually pass out of the Gulf directly through Colville Channel. The net circulation in the Hauraki Gulf is estimated to go from north to south, driven by residual tidal currents (Greig and Proctor 1988; Proctor and Greig 1989; Sharples 1997; Black et al. 2000; Zeldis et al. 2004). The tidal amplitude in the Gulf ranges from ~ 1.35 m in the southern Firth of Thames to ~ 0.85 m in the outer Gulf north of the Barrier Islands (Greig and Proctor 1988). Maximum tidal currents are on average stronger in the three Channels (33–82 cm s^{-1}) compared to the central Gulf (25–42 cm s^{-1}) (Greig 1990) for which predicted average tidal velocities do not exceed ~ 15 cm s^{-1} (Black et al. 2000). The non-tidal circulation is mainly driven by wind, with different wind directions resulting in different current directions. Surface currents are mainly in wind direction, whereas due to strong stratification, subsurface currents form closed circulation cells/gyres in near-coastal areas under SE and NE winds (Proctor and Greig 1989; Black et al. 2000). Proctor and Greig (1989) modelled a steady inflow from the north, representing a mass flux into the Gulf and caused by winds acting on the shelf north of the Gulf.

Manighetti and Carter (1999) considered that the main factor causing sediment redistribution in the Hauraki Gulf was interaction of wind and tidally driven near-bottom currents with waves and oceanic incursions of the East Auckland Current (Fig. 1). According to their model, under calm weather conditions, the circulation is dominated by the tide and the velocities generated are not strong enough to resuspend sand-sized particles. However, under meteorological forcing, large storm waves with the potential to interact with the seafloor down to 100-m water depth lead to reworking of the sediments (Manighetti and Carter 1999). The combination of wave entrainment of sediments and advection by other

wind-induced and tidal currents results in transport of sand across the shelf to the central Gulf. This in turn leads to a net gain of sediments in the central Gulf (sediments from the mainland north of Cape Rodney) and a net loss of sediments from the Western Coromandel Peninsula through Cradock and Colville Channels (Manighetti and Carter 1999).

Hume et al. (2000) examined sediment transport along the shoreward margin of the Jellicoe Channel around Cape Rodney. They obtained near-bed velocity data with acoustic and video monitoring of bedforms at 25-m depth, which included weather conditions ranging from calm to an extratropical storm with significant wave height exceeding 6 m at a peak period of 12 s. Their results confirmed that wave-induced currents reworked surficial sediments and resulted in sediment transport. However, the resulting transport was shore parallel, driven by the strong tidal currents, and not towards the central Gulf as suggested by Manighetti and Carter (1999). The model results of Black et al. (2000) suggest that wave-entrained sediment within the Hauraki Gulf is unlikely to migrate towards the central Gulf, due to the presence of circulation cells that isolate the central Gulf region.

Methods

Sampling

A set of 14 sediment cores was collected in the inner/central Hauraki Gulf (Fig. 1 and Table 1) using a Rumohr-type gravity corer with a total weight of ~ 80 kg and a tube diameter of 100 mm. The Rumohr corer is especially designed to take

Table 1 Site information for the 14 sediment cores from the central Hauraki Gulf taken from aboard the MV Macy Gray (Western Work Boats) on January 28, 2015

Core no. NZ-IC-	Latitude S	Longitude E	Water depth m	Core length cm
1	36° 36.795′	175° 04.107′	44.5	57
2	36° 36.897′	175° 05.963′	45.8	42
3	36° 35.019′	175° 06.256′	47.1	40
4	36° 35.308′	175° 04.131′	44.1	31
5	36° 35.514′	175° 02.321′	45.3	57
6	36° 34.490′	175° 03.724′	44.9	34
7	36° 34.225′	175° 02.237′	45.6	30
8	36° 33.444′	175° 04.054′	45.1	42
9	36° 32.719′	175° 05.646′	46.5	34
10	36° 32.097′	175° 03.689′	45.5	32
11	36° 31.397′	175° 01.767′	46.2	20.5
12	36° 30.308′	175° 05.244′	45.5	13
13	36° 30.374′	175° 02.969′	46.9	23
14	36° 28.697′	175° 02.744′	47.7	20

short, undisturbed sediment cores from the very top sediment layers. Coring was successful and could be done without any loss of material. After retrieval, the 15–57-cm-long sediment cores were sliced into 1-cm-thick subsamples.

Particle size analysis

Particle size analysis was performed with a laser diffraction particle size analyser (Malvern Mastersizer 2000) on all subsamples. Prior to the measurement, the terrigenous sediment fractions were isolated by removing organic carbon and calcium carbonate. Organic carbon was removed by adding 10 ml of 10% hydrogen peroxide in repeated steps until the reaction stopped. Afterwards, the samples were diluted with filtered, demineralised water until a pH-value of ~ 7 was achieved. The calcium carbonate was then removed with 1 ml of 25% solution of hydrochloric acid. Also this step was repeated until the reaction stopped. After re-establishing a pH value of ~ 7, the samples were dispersed with ~ 1 ml of 10% calgon and stirred. The results obtained show the particle size distribution from 0.05 to 2000 μm subdivided into 100 size classes.

XRF analysis

Approximately 1 g of oven-dried subsamples of each sediment slice was ground and homogenised using a mortar and pestle. The powdered samples were loaded into a sample cup, covered with a thin Mylar film, and measured using an Olympus Innov-X Delta 50 keV Handheld XRF Analyser gun (Olympus Innov-X 50KV DP4050CX) set to "Soil Mode" and mounted in a benchtop stand. Concentrations of major and trace elements were recorded by Innov-X Delta Advanced PC software. Scanning time was approximately 90 s per sample. In this study, only the Ca/Ti ratios are shown and discussed as these show the strongest signal. To determine accuracy and precision of the method, an international reference material (Green River Shale, SGR-1) was measured after every 10 samples, with the results indicating consistent values (standard deviation for Ca and Ti within 2% of absolute values).

Radiocarbon dating

To constrain the depositional history of the central Hauraki Gulf within a stratigraphic framework, discrete samples from different depths were selected for accelerator mass spectrometer (AMS ^{14}C) radiocarbon dating. Macroscopic carbonate bivalve and gastropod shell fragments as well as mixed benthic foraminifera (approximately 10 mg picked from the 150–500 μm fraction) were dated at the Poznań Radiocarbon Laboratory, Poland, or at Beta Analytics London, UK (Table 2). All AMS ^{14}C ages were corrected for isotopic

Table 2 Overview of the AMS-^{14}C dates in the sediments based on the analysis of mixed benthic foraminifera (MBF) and carbonate shell fragments (CS)

Core no. NZ-IC	Depth (cm)	Lab. identification	Conventional radiocarbon age (BP)	Sample type	1σ range of calendar years BP	2σ range of calendar years BP	Median probability age (calendar years BP)
1	13–14	Poz-78719	3240 ± 50	MBF	3253–3037	3366–2940	3149
1	26–27	Poz-78720	2705 ± 30	MBF	2543–2373	2729–2369	2514
1	27–28	Poz-75129	8440 ± 40	CS	9238–9051	9353–8957	9146
1	44–45	Poz-78721	7140 ± 50	MBF	7768–7623	7854–7553	7697
1	50–51	Poz-75130	9880 ± 50	CS	11,041–10,797	11,152–10,717	10,924
3	9–10	Poz-78713	1455 ± 30	MBF	1161–1010	1242–963	1093
3	9–10	Poz-75207	485 ± 30	CS	295–127; 78–modern	319–modern	198
3	18–19	Poz-78714	1900 ± 40	MBF	1575–1447	1693–1369	1533
3	36–37	Poz-78715	2830 ± 40	MBF	2773–2578	2812–2450	2663
3	38–39	Poz-75161	4045 ± 35	CS	4263–4056	4371–3960	4166
5	12–13	Poz-75162	8950 ± 30	CS	9772–9595	9917–9559	9703
5	33–34	Poz-75163	7120 ± 35	CS	7738–7618	7815–7549	7678
6	13–14	Poz-75164	485 ± 30	CS	295–127; 68–modern	319–modern	198
7	21–22	Poz-75166	108.54 ± 0.31 pMC	CS	Modern	Modern	> 1950 AD
8	9–10	Beta–455044	1290 ± 30	MBF	982–846	1044–768	914
8	36–37	Beta–455043	2530 ± 30	MBF	2366–2211	2418–2102	2283
9	13–14	Poz-75167	575 ± 30	CS	361–201	460–201; 77–modern	288
9	28–29	Poz-75168	1830 ± 30	CS	1537–1389	1599–1340	1464
14	6–7	Beta–455045	2180 ± 30	MBF	1936–1877	2017–2346	1861
14	18–19	Poz-75169	770 ± 30	CS	556–429	580–359	487

fractionation using δ^{13}C values. The resulting conventional radiocarbon ages were converted into calendar years using the Calib 7.1 software (Stuiver et al. 2017) with the Marine 13 calibration curve (Reimer et al. 2013) considering a global mean reservoir age of 400 years (Bard 1998), which has been confirmed as appropriate for nearby New Zealand east coast marine waters (Higham and Hogg 1995). Results are given as the median probability calendar ages accompanied by the 1σ (68.3% probability) and 2σ ranges (95.4% probability) (Table 2).

SWAN simulation of wave parameters in the Hauraki Gulf

To evaluate the potential role of waves in the distribution of surficial sediments in the Hauraki Gulf, a regional nonstationary SWAN model (*Simulating Waves Nearshore*; http://swanmodel.sourceforge.net) was set up (Zijlema 2010). It simulates the wave field for the northeast region of the North Island over the period 1989–2009. An unstructured grid (27,673 cells) was used with a grid cell size that varies from 50 km^2 offshore (more than 1000-m depth) to 0.5 km^2 in the vicinity of the Hauraki Gulf (depth less than 100 m).

Following Blossier et al. (2016), the model was nested into the global WaveWatch III (WW3) Ocean Wave hindcast model (National Oceanic and Atmospheric Administration, NOAA). Hourly 0.5° spatial resolution winds (Climate Forecast System Reanalysis Reforecast—CFSRR) provided by the NCEP (National Center for Environmental Prediction) drove the global model and were included in the local nested model. Spectral wave conditions applied to the SWAN model boundaries were extracted from the nearest WW3 output locations (seven points). The nonstationary model time step was 30 min and wave field data were generated every hour. Regional bathymetry was provided by NIWA (National Institute for Water and Atmospheric Research, NZ) for New Zealand (Mitchell et al. 2012) and for the Hauraki Gulf (Mackay et al. 2012). The wave model was validated based on the data collected by a wave buoy located near Motiti Island to the southeast of the Coromandel peninsula and maintained by the Bay of Plenty Regional Council. Reasonable hindcasting skill was found for significant wave height H$_s$ (R^2 = 0.85 and RMSE (root-mean-square error) = 0.2) and mean wave period Tm (R^2 = 0.75 and RMSE = 0.9). Wave direction was reasonably simulated as well, with R^2 = 0.60, increasing to 0.75 for the higher waves (H$_s$ > 0.7 m) that are of interest for this study.

Results

Sediment description

All sediment cores consisted of greenish-grey, massive silty sands with abundant shell fragments, occurring either as isolated fragments or concentrated in shell beds (Fig. 2). There were no obvious changes with depth and no structures were observed. Upon slicing of the cores, it became obvious that the northern cores contained more and larger shell fragments, but otherwise visual observation did not reveal any clear trends with depth or with core location. For this reason, the sediment characterisation in this paper focuses on quantitative grain-size analysis and XRF results.

Radiocarbon AMS ^{14}C dating

Twenty radiocarbon dates based on carbonate shell fragments (mussels and snails, $n = 11$) and mixed benthic foraminifera assemblages ($n = 9$) have been measured on 8 out of the total of 14 cores (Table 2). The individual cores are characterised by numerous age reversals. The oldest measured ages go back as far as 10,900 cal years BP (Table 2). In general, the ages from the northern part of the study area span the last ~2300 years, whereas samples from the southern part have ages as old as 11,000 years (Table 2). However, due to the numerous age reversals, an estimation of sedimentation rates is difficult.

Considering solely those ages obtained on mixed benthic foraminiferal samples, these produce a less complex age model with only one reversal in core NZ-IC-1 (Fig. 3). If these ages are taken to be correct, they imply sedimentation rates in the order of a few centimetres per kiloyear. However, given the age reversal in NZ-IC-1 and the evidence of reworking indicated by the numerous other age reversals resulting from the dated shell fragments, these sedimentation rates should be

taken with utmost caution. Nevertheless, despite some age reversals, the two cores NZ-IC-1 and NZ-IC-3, each providing five dates, show a long-term trend of decreasing ages towards the core top (Fig. 3). A similar trend is revealed for cores NZ-IC-8 and NZ-IC-9, however, which are only dated in two levels each.

Particle size analysis

The terrigenous fraction of the sediments in the study area generally consists of very fine to fine sands with varying amounts of finer and coarser particles (Fig. 4). No general trend in particle size with core depth is evident within individual cores (Fig. 5). However, even though the general grain-size distribution follows the same pattern for all the cores (Fig. 4a), values for both the fine fraction (< 10 μm) and the coarse fraction (> 200 μm) reveal a clear distinction between the southern (NZ-IC-1–NZ-IC-7; > 36° 34′ S) and the northern cores (NZ-IC-8–NZ-IC-14; < 36° 34′ S). The average grain-size distribution of northern vs. southern samples (Fig. 4b) further illustrates this differentiation, with generally finer sediments in the south and coarser sediments in the north. Interestingly, in contrast to the fine fractions, where only the amount of material varies between the northern and the southern cores, coarse material > 600 μm is solely present in the northern cores.

The difference between the northern and southern sites can be well illustrated by examining the < 10 μm fraction. In the southern cores (NZ-IC-1–NZ-IC-7), this varies between 11.3 and 40.0 vol-%, with a mean of 20.2 vol-% (SD = 4.4), while in the northern cores (NZ-IC-8–NZ-IC-14), it varies between 6.5 and 23.7 vol-% with a mean of 11.9 vol-% (SD = 2.8) (Fig. 5). In addition, values for the coarse fraction > 300 μm reveal significant differences between southern and northern sediments, with proportions from 0.7 to 9.3 vol-% (mean of 4.5

Fig. 2 **a** Entire sediment column of core NZ-IC-13 with an overall length of 23 cm. **b** Example of a shell bed in core NZ-IC-8 (22-cm core depth). **c** Example of an isolated shell fragment in core NZ-IC-2 (26-cm core depth). The diameter of the core tube is 10 cm

Fig. 3 Radiocarbon dates obtained on eight of the Hauraki Gulf sediment cores
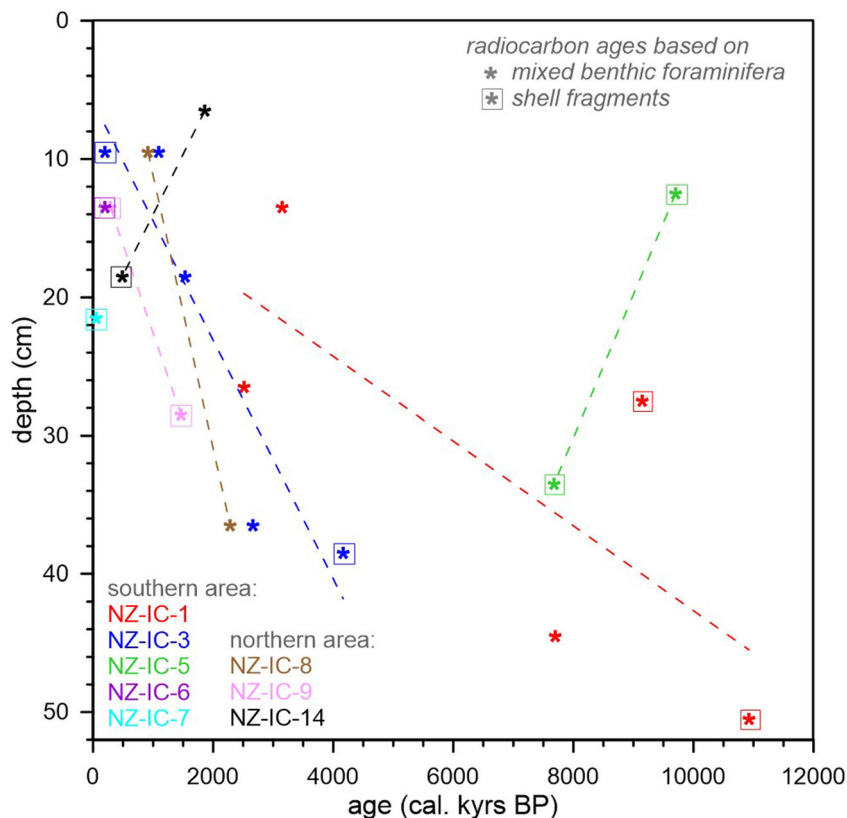
vol-%; SD = 1.9) in the southern cores and from 4.5 to 15.2 vol-% (mean of 10.0 vol-%; SD = 2.2) in the northern cores.

XRF analysis

The XRF analysis indicates no coherent patterns in the cores with depth as exemplified here by the Ca/Ti ratios (Fig. 6). However, as noted above for the particle size analysis, differences can be observed between the sediments in the southern and northern parts of the study area. These differences are

particularly evident for the Ca/Ti ratio, which is often used to distinguish between terrigenous (i.e. Ti) and marine (i.e. Ca) inputs (e.g. Piva et al. 2008; Ingram et al. 2010; Fig. 6).

The Ca/Ti ratios of the northern sediments are twice as high as those of sediments in the southern study area, with mean values of 75.8 and 38.2, respectively. This shows that a distinct N-S divide is not solely a feature of particle size distribution, but also of elemental compositions. However, in contrast to the clear north-south pattern revealed by the grain-size data (NZ-IC-1–NZ-IC-7 vs. NZ-IC-8–NZ-IC-14), the
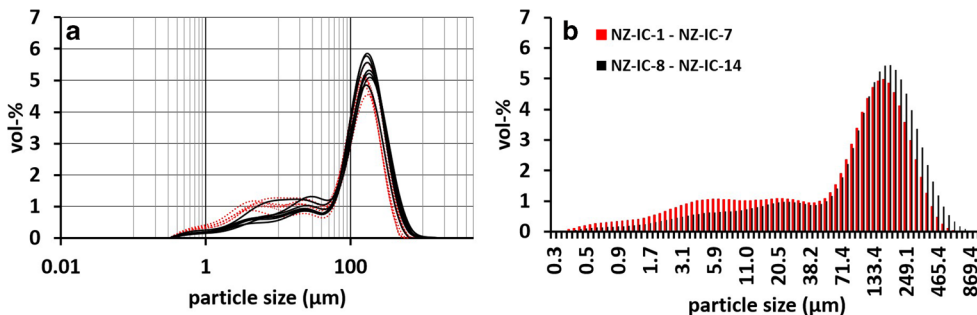

Fig. 4 a Average particle size distributions in each of the 14 sediment cores obtained by averaging the percentages per size class over all individual samples. Red dotted lines indicate the southern (NZ-IC-1–NZ-IC-7), black lines the northern sediment cores (NZ-IC-8–NZ-IC-14). Sediments of the southern cores generally contain a greater proportion of the fine fraction < 20 μm and a lower proportion of

coarser fractions > 200 μm. **b** Bar chart indicating the average grain-size distributions of all southern cores (NZ-IC-1–NZ-IC-7, in red) and all northern cores (NZ-IC-8–NZ-IC-14, in black), again obtained by averaging the average percentages per size class from **a** over the individual cores from the two regions. Major differences are also visible here in the particle size fractions < 20 μm and > 200 μm

Fig. 5 Proportion of the terrigenous fraction with grain-size < 10 μm for each core. Generally, higher proportions of this fine fraction are found in the southern (NZ-IC-1 to NZ-IC-7) compared to the northern cores (NZ-IC-8 to NZ-IC-14). Black shading of the curves indicates proportions above 15 vol.-%. Calendar ages BP are indicated (bold, italic numbers in blue refer to radiocarbon dates obtained on mixed benthic foraminifera; normal grey numbers to those obtained on shell fragments)
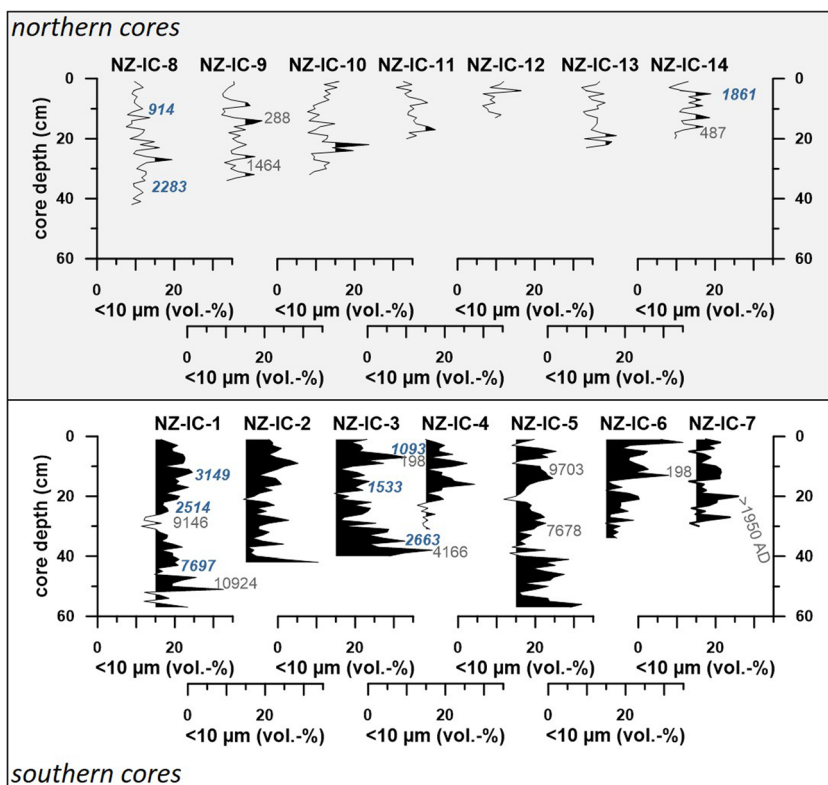
transition from high-to-low Ca/Ti ratios occurs slightly further south (36° 35′ S instead of 36° 34′ S) with NZ-IC-6 and NZ-

IC-7 showing comparably high ratios compatible with a "northern pattern" (Fig. 5).

Fig. 6 Ca/Ti ratio of the sediments, indicating higher ratios in the northern (NZ-IC-8 to NZ-IC-14). Black shading of the curves indicates Ca/Ti ratios over 50
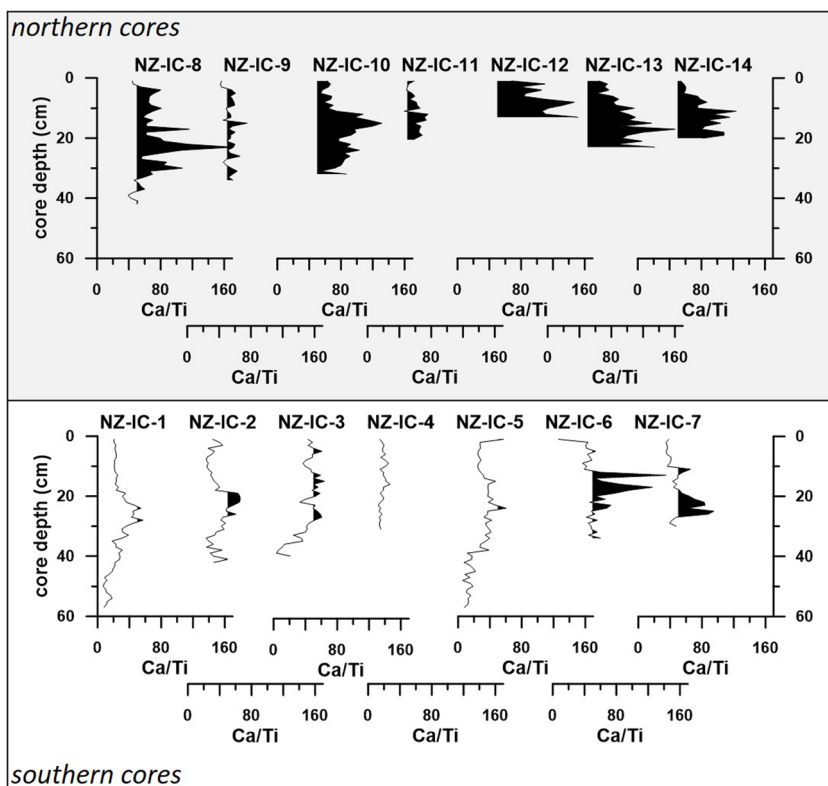
SWAN simulation

The results of the SWAN simulation of wave patterns carried out for the years 1989–2009 indicate that the highest average H_s over this period occurred in the open Pacific Ocean outside the Hauraki Gulf, with a maximum of ~2.3 m in the north-eastern corner of the simulated region (Fig. 7a). Within the Hauraki Gulf, mean H_s decreased southward towards the relatively shallow Firth of Thames. Values range from ~1.1 m in the northern part of the central Hauraki Gulf and the major channels to a minimum of ~0.3 m at the southern end of the Firth of Thames and in sheltered estuaries. Average H_s at the coring sites varied from 0.95 m in the north (NZ-IC-14) to 0.81 m in the south (NZ-IC-2), consistent with this southerly decreasing trend (Fig. 7a). Under strong wind forcing, H_s at the coring sites can reach much higher values. Whereas strong NE and SW winds can result in H_s of 3 to 4 m (Fig. 5b, c), maximum values between 4.7 m (NZ-IC-1) and 5.0 m (NZ-IC-14) appear to be related to easterly storm winds (Fig. 7d).

The gradual decrease in H_s towards the south observed during average conditions also characterises wave height storm conditions (Fig. 7), except in the case of SW storms, when newly generated waves are relatively uniform within the study area (Fig. 7c). The three major channels connecting the Hauraki Gulf with the Pacific Ocean–Jellicoe, Cradock, and Colville Channels—generally experience higher average H_s than other areas in the Hauraki Gulf (Fig. 7). Shadow zones with low mean H_s occur in the lee of the larger Hauraki Gulf Islands (e.g. Little and Great Barrier Island) and on the west coast of the Coromandel Peninsula. Overall, H_s in the study area varied between 0.1 and 5.0 m throughout the simulation period.

The highest H_S in the study area occur during easterly storms. At these times, the largest waves enter the Hauraki Gulf through Colville Channel, producing H_s of up to ~5.0 m in the northern study area, with a strong reduction of H_s towards the south. Differences in H_s between the southernmost and the northernmost coring sites can exceed 1 m (e.g. on the 10th of July 2007, Fig. 7d). After entering the Gulf
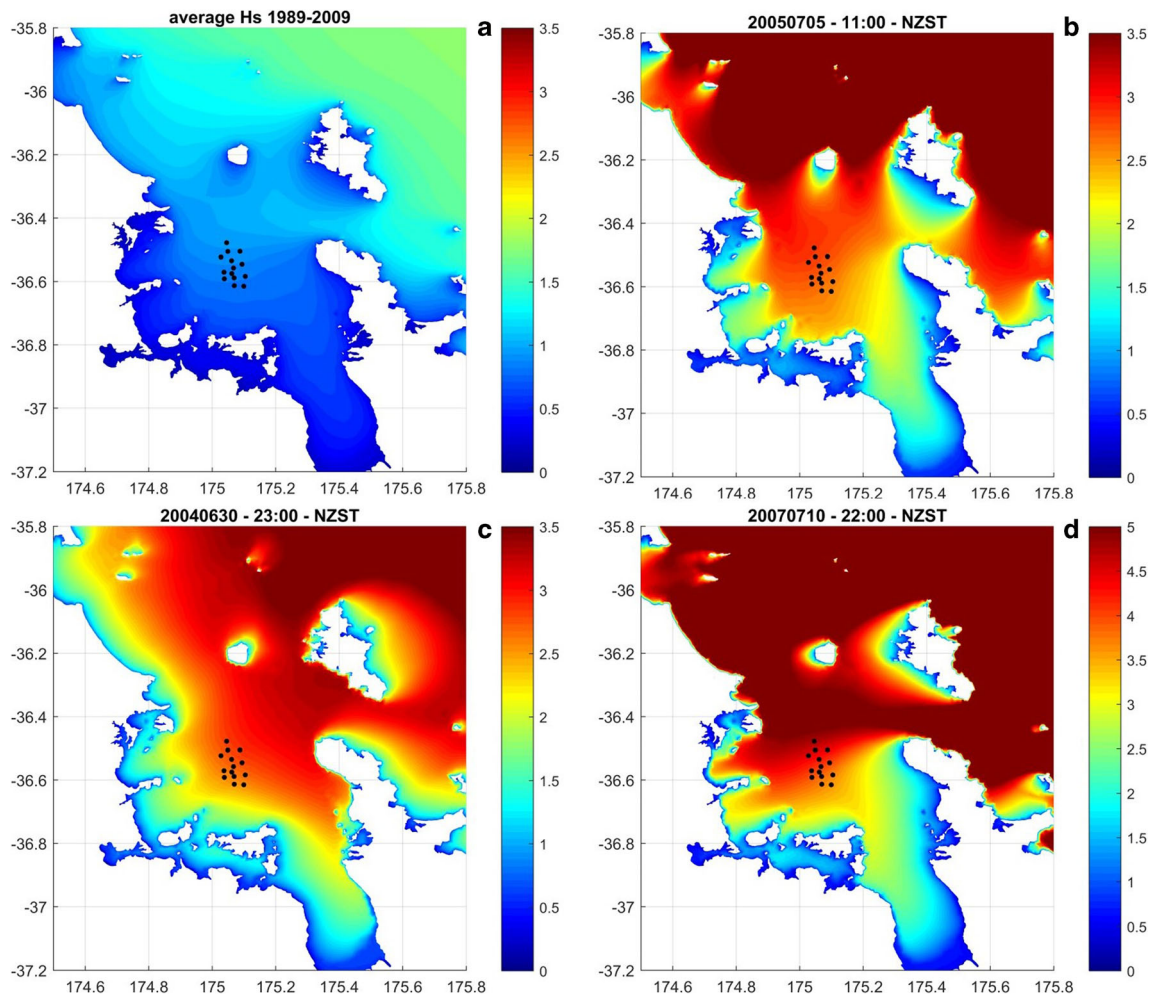

Fig. 7 Maps showing significant wave heights H_s (in m) at different times. **a** Average H_s of the simulated years 1989–2009; **b** H_s on the 5th of July 2005, with waves predominantly coming from the northeast; **c** H_s on the 30th of June 2004, with H_s increasing in NE direction; **d** H_s on the 10th of July 2007, with waves mainly entering via Colville Channel. The core sites are indicated by the black dots

through Colville Channel, waves slowly rotate clockwise towards the northern and anti-clockwise towards the southern Hauraki Gulf. Since the wave energy (mean wave energy density per unit area, J/m^2) is solely dependent on the wave height, the H_s translates directly into wave energy.

Using linear wave theory and threshold of entrainment relationships proposed by Komar and Miller (1973), we calculated the minimum wave conditions required to entrain sediment grains with diameters from 4 to 250 μm at the depths the cores were obtained from. The results indicated that, ignoring cohesion, silt-sized sediment can be entrained during average conditions, while entrainment of sand-sized sediment requires storm conditions with wave heights exceeding 3 m.

Discussion

Low Holocene sediment thickness

The sediment cores studied here were taken from the region identified by Manighetti and Carter (1999) as the main depocenter in the Hauraki Gulf. They estimated post-transgressive sediment thicknesses of up to 10 m in this location. Combining this number with the regional sea-level history indicating the inundation of this area between 11 ka BP (corresponding to a regional sea level of − 46 m, i.e. roughly the depth of the collected sediment cores) and 9 ka (corresponding to a regional sea level of − 24 m, i.e. providing a water depth of ~ 20 m at this site) (Carter et al. 1986) would point to average sedimentation rates on the order of up to 1 m/kyr or even higher if sedimentation only started considerably after the inundation. Any variations in the available accommodation space due to tectonic uplift/subsidence, which could have affected the sedimentation pattern, are unlikely as this region has been tectonically rather stable throughout the Late Quaternary (Williams 1991). However, the new age determinations are characterised by numerous age reversals in the cores (Figs. 3 and 5), a common feature for shallow shelf sediments containing shell fragments or even shell beds (Norris and Grant-Taylor 1989; Gillespie and Nelson 1996). This indicates that sedimentation in the central Hauraki Gulf is not continuous, but characterised by intensive reworking/resedimentation. Furthermore, the presence of datable material with ages of up to ~ 11 ka in the uppermost 60 cm of the cores does not support the assumption of long-term sedimentation rates of up to 1 m/kyr. Although the oldest ages are obtained from carbonate shell fragments, which can easily be reworked, foraminifera also yield ages of > 7 ka and display one age reversal (without considering the shell fragments). If sedimentation rates were up to 1 m/kyr, ages of several thousands of years would not be expected so close to the sediment surface. Furthermore, the overall trends of decreasing ages towards the core tops revealed by 4 out of 6

cores with more than one date (Fig. 3) provide a further hint (not more) to long-term net average sedimentation rates (i.e. ignoring age reversals) on the order of 1 to 10 cm/kyr. The combined evidence of foraminiferal and shell fragment ages and the observation that the rate of burial in this area appears to be close to the rate of reworking strongly suggest that the central Hauraki Gulf is characterised by low average sedimentation rates. This conclusion is consistent with a low modern-day sediment input into the Hauraki Gulf system, mainly contributed by several small rivers, as proposed by Manighetti and Carter 1999. Another possible sediment source could be cliff erosion on the western margin of the Hauraki Gulf, where the erosion of flysch deposits can produce considerable amounts of sediments (de Lange and Moon 2005). However, the sand produced tends to stay in the nearshore at depths shallower than 15 m, whereas the finer sediments are mostly advected out of the Gulf as suggested by satellite images (Hilton and Hesp 1996; Manighetti and Carter 1999).

Today, the small river systems discharge ~ 100 m^3/s to the inner Gulf (Sikes et al. 2009), with the largest suppliers of terrestrial material being the Piako and Waihou Rivers, which both drain igneous and volcanic regions and the predominantly agricultural Hauraki Plains and discharge into the southern end of the Firth of Thames (Fig. 1). Interestingly, after the arrival of first the Polynesian settlers (~ 1000 year BP) and later on the European settlers (~ 1800 AD), soil erosion rates in New Zealand increased due to land clearances (e.g. Bussell 1988; McGlone and Wilmshurst 1999). However, the majority of the soils eroded following these clearances were trapped in estuaries and sheltered near-coastal areas, and thus would not have reached the central Gulf (Carter and Eade 1980; Greig 1982).

These observations, which indicate that overall sedimentation rates are much lower than ~ 1 m/kyr, imply that the depocenter described by Manighetti and Carter (1999) probably only consists of a small component of post-transgressive sediments, and that most of the sediment package, which may be up to 10 m thick, is most likely older. Given that a significantly higher sediment input would have been needed to result in the deposition of this thick package, other sediment sources must have contributed in the past. The prime candidate here is the Waikato River, which flowed into the Hauraki Gulf until ~ 24 ka BP, when it switched to its modern-day course finally discharging into the Tasman Sea in the west (Manville and Wilson 2004) (Fig. 1). Its present-day mean discharge of 340 m^3/s (Duncan and Woods 2004) indicates its potential to deliver several times the amount of sediment of all the modern smaller rivers entering into the Hauraki Gulf combined. If the Waikato River represented an additional sediment source in the past, two scenarios could explain the presumably older deposits observed in the seismic reflection data by Manighetti and Carter (1999): these were deposited (i) as flood plain deposits under Pleistocene sea level low-stand

conditions, e.g. during the last glacial when the Waikato River last drained into the Hauraki Gulf region, or (ii) as marine sediments during the last interglacial when, in contrast to today, sediment input to the Gulf was much higher, and was predominantly supplied by the Waikato River. In both cases, the underlying erosional surface inferred to be linked to the last post glacial transgression (Manighetti and Carter (1999) must be older, possibly even old enough to be linked to the major transgression following the pen-ultimate glaciation.

North-to-south gradient in sediment composition

The latitudinal N-S pattern, visible in both sediment grain sizes and elemental concentrations (Figs. 5 and 6), most likely reflects the influence of the present-day hydrodynamic regime in the study area as a combination of tidal currents, oceanic inflows, and wave-induced currents. Tidal and wave-generated currents have been shown to affect sediment transport in the Hauraki Gulf, whereas especially in greater depths (> 50 m) sediment transport appears to be dominated by strong storm events (Hume et al. 2000). In addition, tidal currents in our working area dominantly flow northward (ebb direction) or southward (flood direction) (Black et al. 2000; Zeldis et al. 2004). Material transported by these tidal currents would be expected to produce similar sediment composition in both parts of the working area. Thus, the strong north-to-south differences in sediment composition within the working area are most likely not caused by tidal currents.

The net overall circulation is dominated by waters entering the Gulf through Jellicoe Channel, flowing anti-clockwise across the Gulf and passing out through Colville Channel in the east (Greig and Proctor 1988; Greig 1990). The dominant influence of the major channels connecting the Hauraki Gulf to the Pacific Ocean can also be seen in the SWAN simulations (Fig. 7). Wave energies in the Gulf are strongest in the channels (Jellicoe, Cradock, and Colville) and then generally decrease from north to south, indicated by on average (for the period 1989–2009) lower mean H_s and, consequently, lower mean absolute wave energies (Fig. 7).

It has been shown previously that storm waves with H_s of ~ 5 m in the Gulf can potentially stir fine sands on the seafloor down to water depths of ~ 100 m (Manighetti and Carter 1999). Under strong storm forcing through Colville Channel (Fig. 7d), when H_s is highest, a steep N-S gradient in wave energy through our sampling area has the potential to modify the seafloor sediments towards the pattern observed in the grainsize and Ca/Ti ratio data (Figs. 5 and 6). Higher wave energies in the north could result in the advection of coarser shell fragments from further offshore, also increasing the Ca/Ti ratio (Fig. 6), and in the resuspension/erosion of finer particles and/or delivery of coarser particles, resulting in a comparably coarser terrigenous sediment fraction (Fig. 5). As the coarser material in the north is marked by a higher shell (i.e. Ca) content (Figs. 6 and 8), the further southward reach of enhanced Ca/Ti ratios compared to the grain-size data might reflect a slightly further southward advection of smaller shell fragments or even abraded carbonate material.

Fig. 8 Examples of wet-sieved particle size fractions > 500 μm in **a** a southern core (NZ-IC-3; 36–37-cm core depth) and **b** northern core (NZ-IC-8; 36–37-cm core depth) indicating the different composition of the coarse fractions between the southern and northern sediments
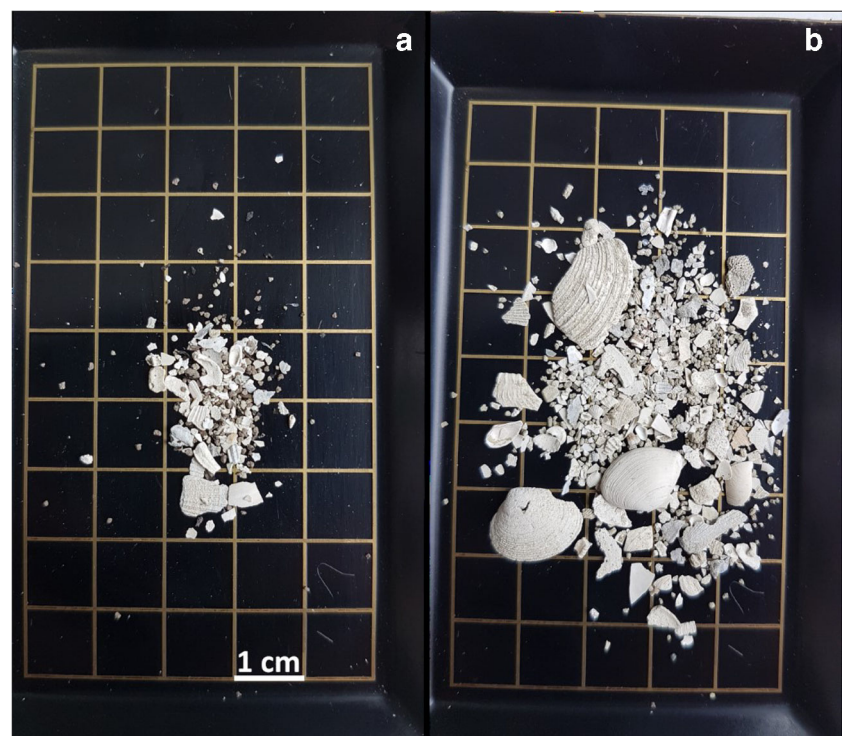
Indeed, strong correlations between latitude, H_s, and grain sizes and elemental composition in the cores can be observed (Table 3) pointing to wave action as one of the important processes affecting grain-size distribution and elemental concentrations (and therefore composition) of the sediments in the central Hauraki Gulf. In a scenario where hydrodynamic conditions are dominated by wave-driven reworking of sediments at the seafloor, the deposition of continuous, undisturbed sedimentary sequences is largely precluded.

Present-day sediment dispersal

Dispersal of sediments in the southern part of the Hauraki Gulf is affected by tidal eddies and water flowing out of the Firth of Thames, whereas the circulation in the northern study area is largely controlled by a seasonally shifting wind field mostly triggering southward or northwestward flowing bottom currents (Zeldis et al. 2004). In addition, this region often is impacted by waters coming through Colville Channel, usually during times of enhanced hydrodynamic forcing (Black et al. 2000). Sikes et al. (2009) assumed that most of the present-day terrigenous sediment input into the Gulf consists of fine-grained material supplied by the Waihou and Piako Rivers to the southern end of the Firth of Thames, from where tidal eddies can transport it to the southern study area. This might explain the higher proportions of fine-grained sediment in this area. However, it would not explain the abrupt change in the fraction < 10 μm observed between the southern and the northern parts of the study site, unless the boundary between the cores NZ-IC-7 and NZ-IC-8 marks the northern-most point to which these fluvial sediments are transported.

Even though an estimation of sedimentation rates based on the radiocarbon dates is difficult due to the numerous age reversals in our sediment cores, there is some indication that

Table 3 Selected correlation coefficients of various sediment parameters, latitude, and average significant wave heights H_s. Strong (> 0.5) positive correlation coefficients are printed in bold, strong negative correlation coefficients (< −0.5) are printed in italics. The data show strong positive correlations between latitude and the proportion of coarser particles > 300 μm, H_s, and Ca/Ti ratios, and strong negative correlations between latitude, H_s, and the proportion of the fine particles < 10 μm, indicating sediment sorting by the hydrodynamic regime. Data used for the correlation: each cm in each core (n = 475) for particle size and Ca/Ti ratio; one value for each core for average Hs and latitude (n = 14)

	Latitude	< 10 μm vol.-%	> 300 μm vol.-%	Average H_s m	Ca/Ti
Latitude	–				
< 10 μm vol.-%	*− 0.59*	–			
> 300 μm vol.-%	**0.70**	− 0.23	–		
Average H_s m	**1.00**	*− 0.58*	**0.68**	–	
Ca/Ti	**0.72**	*− 0.52*	**0.59**	**0.70**	–

the sediments in the northern parts of the study site are younger, spanning only the last 2300 years (288 to 2283 years, n = 6), whereas sediments in the southern part of the study site span the last 10,900 years (recent to 10,924 years, n = 14, 50% of the ages are > 4000 years, Table 2). This points to a peculiar pattern of lower "average sedimentation rates" in the southern part of the study area, where higher relative contributions of finer sediments are interpreted to reflect the deposition of sediments from fluvial sources, compared to the northern sites, where these finer sediments are missing, but where the radiocarbon dates point to higher "average sedimentation rates".

This observation, at first glance contradictory, might be explained by the existence of another sediment source for the northern sites. A hint at the identification of such a source is given by the presence of coarse (> 600 μm) terrigenous materials, which are absent in the southern sediments (Fig. 4), and which occur in combination with much higher Ca contents. Visual inspection of the untreated sediment fraction > 500 μm from a northern (NZ-IC-3) and a southern (NZ-IC-8) sediment sample reveals a much higher content of large shell debris in the north (Fig. 8), which is consistent with the higher proportion of coarse material in the terrigenous sediment fraction in the northern cores (Fig. 4). Thus, higher "average sedimentation rates" in the north might be largely a result of enhanced deposition of coarse materials consisting largely of fragmented carbonates, a typical feature for carbonate-rich temperate shelf deposits (Smith 1992; Smith and Nelson 2003). In addition to local carbonate bioproductivity (foraminifera, bivalve, and gastropods), which probably affects the northern study sites in a similar way to the southern sites, a large proportion of the carbonate shell debris in the north may be relict material transported to the study site. The mostly fragmented nature of the carbonate shells indicates the exposure to rather high energetic settings and supports the idea of the carbonate materials being transported to the study site. Manighetti and Carter (1999) described regions of high carbonate content (up to > 92%) in Hauraki Gulf surface sediments from the Jellicoe and Colville Channels, from north of Tiritiri Matangi Island, and from directly southwest of our southern coring sites. Especially in the Jellicoe and Colville Channels, these sediments consist in large part of shell hash with dominant size modes of up to 350 μm.

During larger storms with waves entering the Gulf through Colville and/or Jellicoe Channel (Fig. 7b, d), carbonate shell hash and coarse terrigenous particles may be resuspended from the seafloor and transported to the study area, resulting in a net gain of coarse material (carbonates and terrigenous material). The ability of storm waves in the Hauraki Gulf to rework coarse carbonate shell fragments, especially in the main channels, has already been outlined in detail by Manighetti and Carter (1999), who also already highlighted the importance of storm events for sediment transport within

the Gulf. The southward weakening of wave energies in the Gulf results in the predominant deposition of this coarse material in the northern part of our study area. Our model reveals a strong N-S gradient in wave energy in our study area for the 10th of July 2007. On this day, waves mainly entered the Gulf via Colville Channel (Fig. 7d). This may suggest that easterly storms are the main driver of coarse sediment input to the central Hauraki Gulf, as this steep gradient would be consistent with the observed N-S differences in sediment composition in the study area.

However, some differences in the location of the major changes in sediment composition occur: for example, the shift from higher to lower Ca/Ti ratios happens between cores NZ-IC-5 and NZ-IC-6, while the shift from lower to higher < 10 μm content occurs between cores NZ-IC-7 and NZ-IC-8. This offset may be explained by an additional input of fine-grained carbonate material to cores NZ-IC-6 and NZ-IC-7 from the southwest during periods of strong westerly winds (e.g. Fig. 7c). Surface sediments in the southwest are characterised by high carbonate (> 50%) and clay (> 30%) contents (Manighetti and Carter 1999).

In terms of sediment accumulation in the central Hauraki Gulf, the younger average age of sediments in the northern part of the study area indicates that the volume of coarse (carbonate and terrigenous) material supplied to the northern study sites is higher than the volume of fine terrigenous material supplied by fluvial processes to the southern study sites, resulting in higher "average sedimentation rates" in the north probably caused by additional supply of coarse-grained material to the northern sites during strong easterly storms. Nevertheless, the sediments in the southern part of the study area are also significantly reworked, as indicated by numerous age reversals.

Conclusions

This study revisited the main sediment depocenter in the central Hauraki Gulf as identified by Manighetti and Carter (1999), focusing on the area with the assumed highest accumulation of > 10 m of post-transgressional sediments, and revealed that this region is in fact controlled by event-driven sediment reworking and input rather than by continuous deposition. This is indicated by radiocarbon ages of up to > 10,000 years obtained on carbonate shell fragments and of up to > 7000 years obtained on foraminifera within the uppermost 60 cm of the sediment. While age reversals in the sedimentary records characterise the entire study area, the sediment composition indicates a differentiation between coarser sediments in the north and finer sediments in the south. We propose that the coarser sediments in the north are—at least partly—supplied under easterly storm forcing from the Colville Channel, whereas the finer sediments in the south

are provided by fluvial input. In terms of average sediment accumulation, the younger average age of sediments in the north indicates that the volume of coarse (carbonate and terrigenous) material supplied to the northern study sites is higher than the volume of fluvial input of fine terrigenous material supplied to the southern study sites. However, reworking dominates over sedimentation in the southern part of the study area as well, as indicated by numerous age reversals in the individual cores. The distinct boundary between these two types of sediment is consistent with a steep gradient in wave energy patterns that can be related to strong easterly storms, and thus the resulting sediments (at least in the north) can be defined as palimpsest sediments.

While the existing conceptual models proposed in the literature argue for modern-day sediment input coming either predominantly from the north or from the south, our new data suggests a combination of both models. Fine fluvial sediments from the south contribute to the sedimentation in the southern study sites and higher inputs of relict carbonate and coarse terrigenous material coming from sources in the east (and in the north) contributes to sedimentation in the northern study sites.

By focusing on a small area with a high spatial resolution in sampling, this study reveals that the general pattern of sedimentation in the Hauraki Gulf previously outlined by Manighetti and Carter (1999) may need some reconsideration. Given that the protection and the sustainable use of coastal ecosystems require a detailed knowledge of the seabed and the processes affecting it, the still limited knowledge of the Hauraki Gulf seabed may cause significant problems for environmental management. Thus, although the Hauraki Gulf is probably the best-studied shelf region of New Zealand, future research efforts should target the sedimentary system of the Hauraki Gulf, the largest shelf embayment of New Zealand.

Compliance with ethical standards

Conflict of interest The authors declare that they have no conflict of interest.

References

Bard E (1998) Geochemical and geophysical implications of the radiocarbon calibration. Geochim Cosmochim Acta 62:2025–2038

Black KP, Bell RG, Oldman JW, Carter GS, Hume TS (2000) Features of 3-dimensional barotropic and baroclinic circulation in the Hauraki Gulf, New Zealand. N Z J Mar Freshw Res 34:1–28

Blossier B, Bryan KR, Daly CJ, Winter C (2016) Nearshore sandbar rotation at single-barred embayed beaches. J Geophys Res Oceans 121:2286–2313

Bussell MR (1988) Mid and late Holocene pollen diagrams and Polynesian deforestation, Wanganui district, New Zealand. N Z J Bot 26:431–451

Carter L, Eade JV (1980) Hauraki sediments. New Zealand Oceanographic Institute Chart. Coastal Series 1:200–000

Carter RM, Carter L, Johnson DP (1986) Submergent shorelines in the SW Pacific: evidence for an episodic post-glacial transgression. Sedimentology 33:629–649

Clement AJH, Whitehouse PL, Sloss CR (2015) An examination of spatial variability in the timing and magnitude of Holocene relative sea-level changes in the New Zealand archipelago. Quat Sci Rev 131:73–101

de Lange WP, Moon VG (2005) Estimating long-term cliff recession rates from shore platform widths. Eng Geol 80:292–301

Dougherty AJ, Dickson ME (2012) Sea level and storm control on the evolution of a chenier plain, Firth of Thames, New Zealand. Mar Geol 307:58–72

Duncan M, Woods R (2004) Flow regimes. In: Harding JS, Mosley MP, Pearson CP, Sorrell BK (eds) Freshwaters of New Zealand. New Zealand hydrological society and New Zealand limnological society, Christchurch, pp 7.1–7.14

Eade JV (1974) Poor knights sediments. New Zealand Oceanographic Institute Chart, Coastal Series 1:200,000

Gillespie JL, Nelson CS (1996) Distribution and control of mixed terrigenous-carbonate surficial sediment facies, Wanganui shelf, New Zealand. N Z J Geol Geophys 39:533–549

Greig DA (1982) Sediments and recent geological history of the Hauraki Gulf, Firth of Thames and Colville Channel, North Island, New Zealand. PhD Thesis, University of Auckland

Greig MJ (1990) Circulation in the Hauraki Gulf, New Zealand. N Z J Mar Freshw Res 24:141–150

Greig MJ, Proctor R (1988) A numerical model for the Hauraki Gulf, New Zealand. N Z J Mar Freshw Res 22:379–390

Griffiths GA, Glasby GP (1985) Input of river-derived sediment to the New Zealand continental shelf: I. Mass. Estuar Coast Shelf Sci 21:773–787

Hicks DM, Shankar U, McKerchar AI, Basher L, Lynn I, Page M, Jessen M (2011) Suspended sediment yields from New Zealand rivers. J Hydrol N Z 50:81–142

Higham TFG, Hogg AG (1995) Radiocarbon dating of prehistoric shell from New Zealand and calculations of the ∆R value using fish otoliths. Radiocarbon 37:409–416

Hilton MJ, Hesp P (1996) Determining the limits of beach-nearshore sand systems and the impact of offshore coastal sand mining. J Coast Res 12:496–519

Hochstein MP, Nixon IM (1979) Geophysical study of the Hauraki Depression, North Island, New Zealand. N Z J Geol Geophys 22:1–19

Hochstein MP, Tearney K, Rawson S, Davey FJ, Davidge S, Henry S, Backshall D (1986) Structure of the Hauraki Rift, New Zealand. R Soc N Z Bull 24:333–348

Howarth RW, Anderson DB, Cloern JE, Elfring C, Hopkinson CS, Lapointe B, Maloney TJ, Marcus N, McGlathery K, Sharpley AN, Walker D (2000) Issues in ecology: nutrient pollution in coastal rivers, bays, and seas. United States Geological Survey. http://pubs.er.usgs.gov/publication/70174406ER

Hume TM, Oldman JW, Black KP (2000) Sediment facies and pathways of sand transport about a large deep water headland, Cape Rodney, New Zealand. N Z J Mar Freshw Res 34:695–717

Ingram WC, Meyers SR, Brunner CA, Martens CS (2010) Late Pleistocene-Holocene sedimentation surrounding an active seafloor gas-hydrate and cold-seep field on the Northern Gulf of Mexico slope. Mar Geol 278:45–53

Komar PD, Miller MC (1973) The threshold of sediment movement under oscillatory water waves. J Sediment Petrol 43:1101–1110

Mackay KA, Mackay EJ, Neil HL, Mitchell JS, Bardsley SA (2012) Hauraki gulf. NIWA chart, miscellaneous series 91

Manighetti B, Carter L (1999) Across-shelf sediment dispersal, Hauraki Gulf, New Zealand. Mar Geol 160:271–300

Manville V, Wilson CJN (2004) The 26.5 ka Oruanui eruption, New Zealand: a review of the roles of volcanism and climate in the post-eruptive sedimentary response. N Z J Geol Geophys 47:525–547

McGlone MS, Wilmshurst JM (1999) Dating initial Maori environmental impact in New Zealand. Quat Int 59:5–16

Mitchell JS, Mackay KA, Neil HL, Mackay EJ, Pallentin A, Notman P (2012) Undersea New Zealand, 1:5,000,000. NIWA Chart, Miscellaneous Series 92

Norris RM, Grant-Taylor TL (1989) Late Quaternary shellbeds, western shelf, New Zealand. J Geol Geophys 32:343–356

Piva A, Asioli A, Schneider RR, Trincardi F, Andersen N, Colmenero-Hidalgo E, Dennielou B, Flores JA, Vigliotti L (2008) Climatic cycles as expressed in sediments of the PROMESS1 borehole PRAD1-2, central Adriatic, for the last 370 ka: 1. Integrated stratigraphy. Geochem Geophys Geosyst 9:Q01R01. https://doi.org/10.1029/2007GC001713

Pocknall DT, Gregory MR, Greig DA (1989) Palynology of core 80/20 and its implications for understanding Holocene sea level changes in the Firth of Thames. New Zealand. J R Soc N Z 19:171–179

Proctor R, Greig MJ (1989) A numerical model investigation of the residual circulation in the Hauraki Gulf, New Zealand. N Z J Mar Freshw Res 23:421–442

Reimer PJ, Bard E, Bayliss A, Beck JW, Blackwell PG, Ramsey CB, Buck CE, Cheng H, Edwards RL, Friedrich M, Grootes PM, Guilderson TP, Haflidason H, Hajdas I, Hatté C, Heaton TJ, Hoffmann DL, Hogg AG, Hughen KA, Kaiser KF, Kromer B, Manning SW, Niu M, Reimer RW, Richards DA, Scott EM, Southon JR, Staff RA, Turney CSM, van der Plicht J (2013) IntCal13 and Marine13 radiocarbon age calibration curves 0–50,000 years cal BP. Radiocarbon 55:1869–1887

Schofield JC (1970) Coastal sands of Northland and Auckland. N Z J Geol Geophys 13:767–824

Sharples J (1997) Cross-shelf intrusion of subtropical water into the coastal zone of Northern New Zealand. Cont Shelf Res 17:835–857

Sikes EL, Nodder SD, Howard ME (2009) Sources of organic matter in a coastal marine environment: evidence from n-alkanes and their δ13C distributions in the Hauraki Gulf, New Zealand. Mar Chem 113:149–163

Smith AM (1992) Aspects of the sedimentology of New Zealand bryozoans and mixed carbonate–clastic deposits: a contribution to the temperate shelf carbonate model Unpublished PhD Thesis, University of Waikato, 469 pp.

Smith VH (2003) Eutrophication of freshwater and coastal marine ecosystems a global problem. Environ Sci Pollut Res 10:126–139

Smith AM, Nelson CS (2003) Effects of early sea-floor processes on the taphonomy of temperate shelf skeletal carbonate deposits. Earth Sci Rev 63:1–31

Stuiver M, Reimer PJ, Reimer RW (2017) CALIB 7.1 [WWW program] at http://calib.org

Thrasher GP (1986) Basement structure and sediment thickness beneath the continental shelf of the Hauraki Gulf and offshore Coromandel region, New Zealand. N Z J Geol Geophys 29:41–50

Uhle ME, Sikes EL, Nodder SD, Pilditch CA (2007) Sources and diagenetic status of organic matter in the Hauraki Gulf, New Zealand: evidence from the carbon isotopic composition of D- and L-amino acids. Org Geochem 38:440–457

Waycott M, Duarte CM, Carruthers TJ, Orth JR, Dennison WC, Olyarnik S, Calladine A, Fourqurean JW, Heck KL, Hughes AR, Kendrick GA, Kenworthy WJ, Short FT, Williams SL (2009) Accelerating loss of seagrasses across the globe threatens coastal ecosystems. Proc Natl Acad Sci 106:12377–12381

Williams PW (1991) Tectonic geomorphology, uplift rates and geomorphic response in New Zealand. Catena 18:439–452

Zeldis JR, Walters RA, Greig MJN, Image K (2004) Circulation over the North-Eastern New Zealand continental slope, shelf and adjacent Hauraki Gulf, during spring and summer. Cont Shelf Res 24:543–561

Zijlema M (2010) Computation of wind-wave spectra in coastal waters with SWAN on unstructured grids. Coast Eng 57:267–277